

# APPLICATION OF BESSEL FUNCTIONS AND DISCRETE FOURIER TRANSFORM TO THE ANALYSIS OF ELECTROMAGNETIC FIELD OF AXIAL SYMMETRY IN C++

PROFESOR BERNARD BARON, PL.

DR. ING. JOANNA KOLAŃSKA-PLUSKA, PL.

**Abstract:** In the work presented an algorithm for evaluation of inverse Discrete Fourier Transform (DFT) and Bessel functions have been elaborated with the purpose of determining of the time – harmonic electromagnetic field distribution in a quasi-3D system with rotational symmetry. An object-oriented programming in C++ language is used for an implementation of a computational algorithm.

**Key words:** *Elektromagnetic Field, Fourier transform*

## INTRODUCTION

In the paper the application of certain modification of inverse Discrete Fourier Transform and the FFT algorithm to the analysis of harmonic electromagnetic field of axial symmetry. The computer program has been elaborated in C++ programming language. A program class has been defined with the methods designed for characterisation of the computers of the magnetic and the electric field by their Fourier transform.

### 1. EQUATIONS OF THE TIME-HARMONIC ELECTROMAGNETIC FIELD OF THE SYSTEM COMPRISED FROM ANNULAR CYLINDER AND A COIL WOUND ON IT.

Consider a current-driven coil is represented by the surface current of angular frequency  $\omega$  and density  $\underline{J}(r, z) = \mathbf{1}_\varphi J_\varphi(r, z)$ .

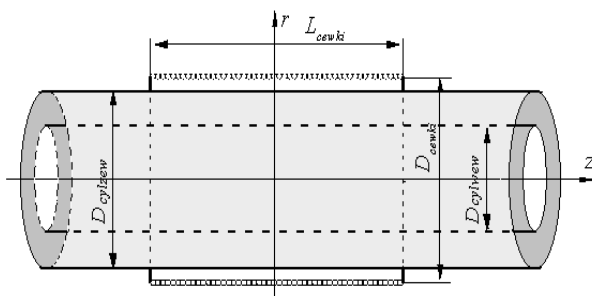


Fig. 1. A current-driven coil represented by the surface current and concentrically placed conducting ring.

The conducting ring, having the conductivity and the permeability is placed concentrically with the solenoid. The whole problem has the following description. In the non-conducting regions the magnetic vector potential  $\underline{A}(r, z) = \mathbf{1}_\varphi \underline{A}_\varphi(r, z)$  fulfills the following equation [1]:

$$\frac{\partial^2 \underline{A}_\varphi(r, z)}{\partial r^2} + \frac{1}{r} \frac{\partial \underline{A}_\varphi(r, z)}{\partial r} - \frac{\underline{A}_\varphi(r, z)}{r^2} + \frac{\partial^2 \underline{A}_\varphi(r, z)}{\partial z^2} = 0 \quad (1)$$

In the paper [4] the Fourier Transforms of the magnetic and electric field strength components, in the region of coil and outside it, have been presented.

In the conducting regions the equation for the magnetic vector potential has the form [1]:

$$\frac{\partial^2 \underline{A}_\varphi(r, z)}{\partial r^2} + \frac{1}{r} \frac{\partial \underline{A}_\varphi(r, z)}{\partial r} - \left( j\alpha^2 - \frac{1}{r^2} \right) \underline{A}_\varphi(r, z) + \frac{\partial^2 \underline{A}_\varphi(r, z)}{\partial z^2} = 0$$

where  $\alpha^2 = \omega\mu\gamma$ . (2)

The solution of the above partial differential equation has been obtained by means of performing the Fourier transform of the magnetic vector potential in  $z$  direction.

$$A(r, \xi) = F_z \{ \underline{A}_\varphi(r, z) \} = \int_{-\infty}^{+\infty} \underline{A}_\varphi(r, z) e^{-j\xi z} dz \quad (3)$$

Work [4] describes in details how the solution of this equation is obtained.

## 2. NOTES ON THE PROBLEM SOLUTION

The current of angular frequency  $\omega$  of the coil creates the distribution of the electromagnetic field of the same frequency, and this in turn induces the eddy currents in conducting material [3]. The magnetic vector potential is determined in four different regions:

$$\underline{A}_\varphi^{(1)}(r, \xi) = F_1(\xi)I_1(r\xi) + F_4(\xi)K_1(r\xi) \quad \text{for } R_{cewki} \geq r > R_{cylzew} \quad (4)$$

$$\underline{A}_\varphi^{(2)}(r, \xi) = F_3(\xi)I_1(pr) + F_6(\xi)K_1(pr) \quad \text{for } R_{cylzew} \leq r \leq R_{cylzew}$$

where  $p = \sqrt{\xi^2 + j\omega\mu\gamma}$

$$\underline{A}_\varphi^{(3)}(r, \xi) = F_2(\xi)K_1(r\xi) \quad \text{for } r \geq R_{cewki} \quad (6)$$

$$\underline{A}_\varphi^{(4)}(r, \xi) = F_5(\xi)I_1(r\xi) \quad \text{for } 0 \leq r \leq R_{cylzew} \quad (7)$$

where  $F_1(\xi)$ ,  $F_2(\xi)$ ,  $F_3(\xi)$ ,  $F_4(\xi)$ ,  $F_5(\xi)$ ,  $F_6(\xi)$  are determined using the following continuity conditions:  
1 for tangential component of electromagnetic field strength and so the magnetic potential as well as for the magnetic field strength at the interface boundary limited by  $R_{cylzew}$ ,

$$\underline{A}_\varphi^{(2)}(r, z) \Big|_{r=R_{cylzew}} = \underline{A}_\varphi^{(4)}(r, z) \Big|_{r=R_{cylzew}} \quad (8)$$

$$\underline{H}_z^{(2)}(r, z) \Big|_{r=R_{cylzew}} = \underline{H}_z^{(4)}(r, z) \Big|_{r=R_{cylzew}} \quad (9)$$

2 for tangential component of electromagnetic field strength and so the magnetic potential as well as for the magnetic field strength at the interface boundary limited by  $R_{cylzew}$

$$\underline{A}_\varphi^{(2)}(r, z) \Big|_{r=R_{cylzew}} = \underline{A}_\varphi^{(1)}(r, z) \Big|_{r=R_{cylzew}} \quad (10)$$

$$\underline{H}_z^{(2)}(r, z) \Big|_{r=R_{cylzew}} = \underline{H}_z^{(1)}(r, z) \Big|_{r=R_{cylzew}} \quad (11)$$

3 for tangential component of electric field strength at the interface boundary limited by  $R_{cewki}$ .

$$\underline{A}_\varphi^{(1)}(r, z) \Big|_{r=R_{cewki}} = \underline{A}_\varphi^{(3)}(r, z) \Big|_{r=R_{cewki}} \quad (12)$$

Additionally the discontinuity condition at the same interface boundary, of the following form, was used:

$$\underline{H}_z^{(1)}(r, z) \Big|_{r=R_{cewki}} - \underline{H}_z^{(3)}(r, z) \Big|_{r=R_{cewki}} = j(z) \quad (13)$$

Using equations (8) - (13) yields in the following system:

$$\begin{aligned} -F_3(\xi)I_1(pR_{rw}) + F_5(\xi)I_1(\xi R_{rw}) - F_6(\xi)K_1(pR_{rw}) &= 0 \\ F_1(\xi)I_1(\xi R_{rz}) - F_3(\xi)I_1(pR_{rz}) + F_4(\xi)K_1(\xi R_{rw}) - \\ &- F_6(\xi)K_1(pR_{rz}) = 0 \end{aligned}$$

$$\begin{aligned} F_1(\xi)I_1(\xi R_{cew}) - F_2(\xi)K_1(\xi R_{cew}) + F_4(\xi)K_1(\xi R_{cew}) &= 0 \\ p\gamma_0\gamma_w F_3(\xi)I_0(pR_{rw}) - \xi\gamma_0 F_5(\xi)I_0(\xi R_{rw}) - \\ &- p\gamma_0\gamma_w F_6(\xi)K_0(pR_{rw}) = 0 \end{aligned}$$

$$\begin{aligned} -\xi\gamma_0 F_1(\xi)I_0(\xi R_{rz}) + \frac{p}{\mu_0\mu_w} F_3(\xi)I_0(pR_{rz}) + \\ + \xi\gamma_0 F_4(\xi)K_0(\xi R_{rw}) - p\gamma_0\gamma_w F_6(\xi)K_0(pR_{rz}) &= 0 \\ \xi\gamma_0 \cdot F_1(\xi)I_0(\xi R_{cew}) + \xi\gamma_0 \cdot F_2(\xi)K_0(\xi R_{cew}) - \xi\gamma_0 \cdot \\ F_4(\xi)K_0(\xi R_{cew}) &= J(\xi) \end{aligned} \quad (14)$$

The above system of equations was solved using the method of pseudosolution based on the orthogonal multiplications.

### 3. APPLICATION OF DFT FOR DETERMINATION OF THE ELECTROMAGNETIC FIELD DISTRIBUTION

In the program the components of electromagnetic field ( $\underline{E}_\varphi$ ,  $\underline{H}_z$ ,  $\underline{H}_r$ ) in the corresponding regions are determined as well the flux of complex Poynting vector.

The elaborated algorithm was tested on the following problem. The coil has length of  $l_c = 500[mm]$ , diameter of  $D_c = 250[mm]$ , and consists of  $w_c = 100$  turns. Each turn carries current of  $I = 10[A]$ ,  $f = 1000[Hz]$ . The conducting ring has the diameter of  $D_{cylzew} = 180[mm]$  and  $D_{cylzew} = 200[mm]$  the relative permeability  $\mu_w = 200$  and the conductivity  $\gamma = 8[MS/m]$ .

In this work we only present the plot of an absolute value of  $P_r^2(r, z)$  component of the Poynting vector over the surface of the cylinder (see Fig.2), the Fourier transforms value of  $\underline{H}_z^{(2)}(r, z)$  (see Fig.3), and the Fourier transforms value of  $\underline{H}_z^{(3)}(r, z)$  (see Fig.4),

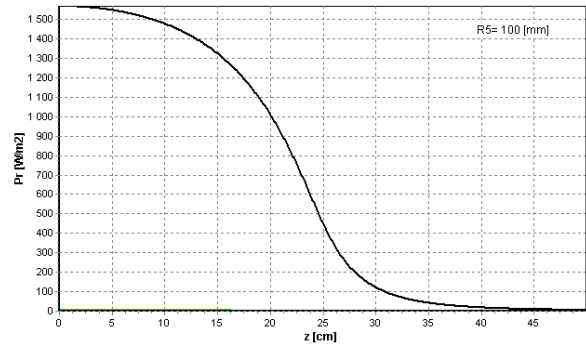


Fig. 2 The absolute value of  $P_r^2(r, z)$  component of the Poynting vector

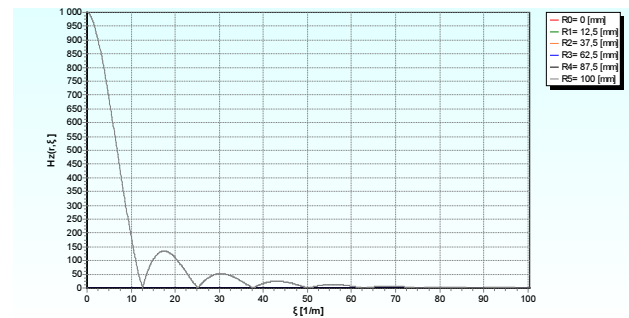


Fig. 3 The Fourier transforms value of  $\underline{H}_z^{(2)}(r, z)$

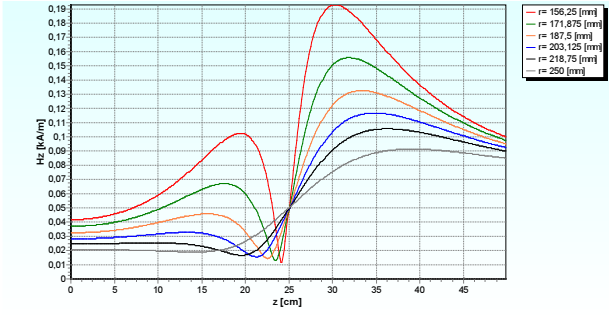


Fig. 4 The Fourier transforms value of  $H_z^{(s)}(r, z)$

The value of real part of flux penetrating cylinder P equals to 302,013 Watt, whereas the value of imaginary part Q, to 302,616 Var.

#### 4. EQUATIONS OF THE TIME-HARMONIC ELECTROMAGNETIC FIELD OF THE SYSTEM COMPRISING FROM CONDUCTING CYLINDER AND A COIL WOUND ON IT.

Consider a current-driven coil is represented by the surface current of angular frequency  $\omega$  and density  $\underline{J}(r, z) = \mathbf{1}_\varphi \underline{J}_\varphi(r, z)$ . The conducting cylinder, having the conductivity  $\gamma$  and the permeability  $\mu$  concentrically with the solenoid. The whole problem has the following description.

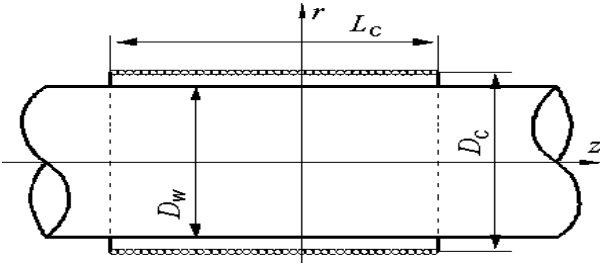


Fig. 5. A current-driven coil represented by the surface current and concentrically placed conducting cylinder.

In the non-conducting regions the magnetic vector potential  $\underline{A}(r, z) = \mathbf{1}_\varphi \underline{A}_\varphi(r, z)$  fulfills the following equation (15):

$$\frac{\partial^2 \underline{A}_\varphi(r, z)}{\partial r^2} + \frac{1}{r} \frac{\partial \underline{A}_\varphi(r, z)}{\partial r} - \frac{\underline{A}_\varphi(r, z)}{r^2} + \frac{\partial^2 \underline{A}_\varphi(r, z)}{\partial z^2} = 0 \quad (15)$$

In the paper [4,5] the Fourier Transforms of the magnetic and electric field strength components, in the region of coil and outside it, have been presented.

In the conducting regions the equation for the magnetic vector potential has the form [1]:

$$\frac{\partial^2 \underline{A}_\varphi(r, z)}{\partial r^2} + \frac{1}{r} \frac{\partial \underline{A}_\varphi(r, z)}{\partial r} - \left( j\alpha^2 - \frac{1}{r^2} \right) \underline{A}_\varphi(r, z) + \frac{\partial^2 \underline{A}_\varphi(r, z)}{\partial z^2} = 0 \quad \text{Fig. 6.}$$

$$\text{where } \alpha^2 = \omega\mu\gamma. \quad (16)$$

The solution of the above partial differential equation has been obtained by means of performing the Fourier transform of the magnetic vector potential in z direction.

$$A(r, \xi) = F_z \left\{ \underline{A}_\varphi(r, z) \right\} = \int_{-\infty}^{+\infty} \underline{A}_\varphi(r, z) e^{-j\xi z} dz \quad (17)$$

Work [4] describes in details how the solution of this equation is obtained.

#### 5. NOTES ON THE PROBLEM SOLUTION

The current of angular frequency  $\omega$  of the coil creates the distribution of the electromagnetic field of the same frequency, and this in turn induces the eddy currents in conducting cylinder [3]. The magnetic vector potential  $\underline{A}_\varphi^{(m)}(r, z)$  and the z component of the magnetic field  $\underline{H}_z^{(m)}(r, z)$  were determined in three different regions. In order to distinguish between appropriate electric and magnetic components the following notation was introduced. In the air-gap between cylinder and coil the superscript  $m=1$  was used,  $m=2$  and  $m=3$  inside cylinder and outside coil, respectively. The knowledge of the electromagnetic field distribution allowed for determination of Poynting vector, which is of special importance in the conducting cylinder.

$$\underline{P}_r^{(m)}(r, z) = \underline{E}_\varphi^{(m)}(r, z) \underline{H}_z^{(m)}(r, z) \quad (m=1,2,3) \quad (18)$$

When using inverse DFT the integration with respect to  $\xi$  is performed in the range from zero to infinity, and it is thus necessary to know all the functions integrated and also the Fourier transforms of the electric and magnetic field strength in all regions considered. This information provides a more practical hint on how the finite integration bounds can be determined.

#### 6. APPLICATION OF DFT FOR DETERMINATION OF THE ELECTROMAGNETIC FIELD DISTRIBUTION

The elaborated algorithm was tested on the following problem. The coil has length of  $l_c = 500[\text{mm}]$ , diameter of  $D_c = 250[\text{mm}]$ , and consists of  $w_c = 100$  turns. Each turn carries current of  $I=10 [\text{A}]$ ,  $f=5000[\text{Hz}]$ . The conducting cylinder has the diameter of  $D_w = 200[\text{mm}]$ , the relative permeability  $\mu_w = 200$  and the conductivity  $\gamma = 8[\text{MS} / \text{m}]$ . The range of integration is restricted to  $\xi_{\max} = 100$ . The analytical description of the absolute value of the z component of the magnetic field strength has the form:  $\underline{H}_z^{(2)}(r, \xi) = \frac{P}{\mu} F_3(\xi) I_0(pr)$  for  $0 \leq r \leq R_w$ ,

where  $p = \sqrt{\xi^2 + j\omega\mu\gamma}$  and  $I_0$  – is modified Bessel function of 0-th order.  $\underline{H}_z^{(2)}(r, \xi)$  is shown plotted in

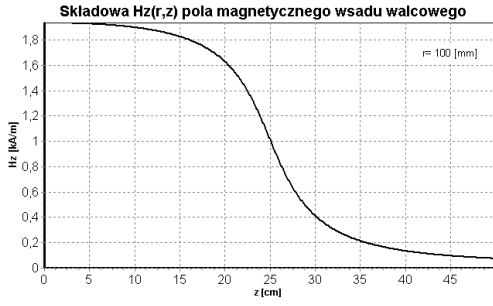


Fig. 6 The absolute value of the  $z$ -th component of the magnetic field strength  $\underline{H}_z^{(2)}(r, z)$

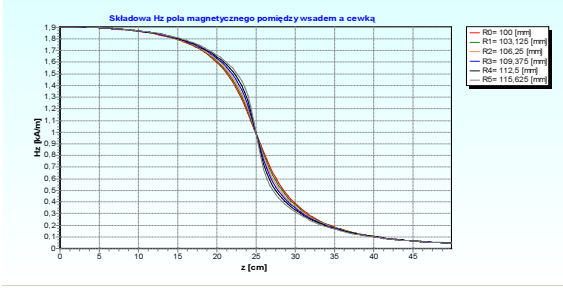


Fig. 7 The absolute value of component of the magnetic field  $\underline{H}_z^{(1)}(r, z)$

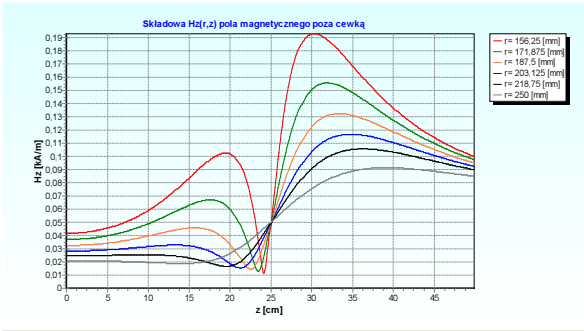


Fig. 8 The absolute value of component of the magnetic field  $\underline{H}_z^{(3)}(r, z)$

The others of components of the magnetic field  $\underline{H}_z^{(1)}(r, z)$  and  $\underline{H}_z^{(3)}(r, z)$  shown Fig 7 and Fig 8.

Next, accordingly to the conception of the modification of the DFT given in [4], the lengths  $\Delta\xi$ ,  $\Delta\varphi$ , and the numbers  $N_\xi$  and  $N_z$  of the integration steps are selected so that  $z_k \xi_l = \Delta\varphi i$ , where  $i = kl$ ;  $z_k = k\Delta z$ ;  $\xi_l = l\Delta\xi$ ;  $k = 0, 1, 2, \dots, N_z$ ;  $l = 0, 1, 2, \dots, N_\xi$ . The following vectors are evaluated when the discretisation is done.

$$\underline{E}_{l\varphi}^{(2)} = \frac{\Delta\xi}{\pi} \underline{E}_\varphi^{(2)}(r, \xi_l) = \frac{-j\omega\Delta\xi}{\pi} F_3(\xi_l) I_1(rp) \quad (19)$$

$$\underline{H}_{lz}^{(2)} = \frac{\Delta\xi}{\pi} \underline{H}_z^{(2)}(r, \xi_l) = \frac{\Delta\xi p}{\mu_0 \mu_w \pi} F_3(\xi_l) I_0(rp) \quad (20)$$

$$\underline{H}_{lr}^{(2)} = \frac{j\Delta\xi}{\pi} \underline{H}_r^{(2)}(r, \xi_l) = \frac{\Delta\xi}{\mu_0 \mu_w \pi} \xi_l F_3(\xi_l) I_1(rp) \quad \text{for } 0 \leq r \leq R_W \quad (21)$$

$$\underline{E}_{l\varphi}^{(1)} = \frac{\Delta\xi}{\pi} \underline{E}_\varphi^{(1)}(r, \xi_l) = \frac{-j\omega\Delta\xi}{\pi} \left[ F_4(\xi_l) K_1(\xi_l r) + \right] \quad (22)$$

$$\underline{H}_{lz}^{(1)} = \frac{\Delta\xi}{\pi} \underline{H}_z^{(1)}(r, \xi_l) = \frac{\Delta\xi}{\mu_0 \pi} \xi_l \left[ F_1(\xi_l) I_0(\xi_l r) - F_4(\xi_l) K_0(\xi_l r) \right] \quad (24)$$

$$\underline{H}_{lr}^{(1)} = \frac{j\Delta\xi}{\pi} \underline{H}_r^{(1)}(r, \xi_l) = \frac{\Delta\xi}{\mu_0 \pi} \xi_l \left[ F_4(\xi_l) K_1(\xi_l r) + F_1(\xi_l) I_1(\xi_l r) \right]$$

for  $R_W < r \leq R_C$  (25)

$$\underline{E}_{l\varphi}^{(3)} = \frac{\Delta\xi}{\pi} \underline{E}_\varphi^{(3)}(r, \xi_l) = \frac{-j\omega\Delta\xi}{\pi} F_2(\xi_l) K_1(\xi_l r) \quad (26)$$

$$\underline{H}_{lz}^{(3)} = \frac{\Delta\xi}{\pi} \underline{H}_z^{(3)}(r, \xi_l) = \frac{-\Delta\xi}{\mu_0 \pi} \xi_l F_2(\xi_l) K_0(\xi_l r) \quad (27)$$

$$\underline{H}_{lr}^{(3)} = \frac{j\Delta\xi}{\pi} \underline{H}_r^{(3)}(r, \xi_l) = \frac{\Delta\xi}{\mu_0 \pi} \xi_l F_2(\xi_l) K_1(\xi_l r) \quad \text{for } r \geq R_C \quad (28)$$

where  $I_0$ ,  $I_1$ ,  $K_0$ ,  $K_1$  are modified Bessel and Kelvin functions, respectively and  $F_1(\xi_l), F_2(\xi_l), F_3(\xi_l), F_4(\xi_l)$  are the integration constants. To determine the integration constants the continuity conditions of the tangential component of the electric field strength were used (and so the continuity of the magnetic vector potential) as well as the magnetic field strength at region interfaces in  $R_W$  direction.

Forming out of these vectors for a given radius  $r$  allows for determination of the following distributions of the electric and the magnetic field quantities and the Poynting vector with respect to previously chosen discretisation points  $z_k = k\Delta z$  ( $k=1, \dots, N_z$ ):

$$\underline{E}_\varphi^{(m)}(r, z_k), \underline{H}_z^{(m)}(r, z_k), \underline{H}_r^{(m)}(r, z_k),$$

$$\underline{P}_r^{(m)}(r, z_k) = \underline{E}_\varphi^{(m)}(r, z_k) \cdot \underline{H}_z^{*(m)}(r, z_k) \quad \text{where } m=1, 2 \text{ or } 3.$$

## 7. REFERENCES

- [1] Krakowski M.: Elektrotechnika teoretyczna. Tom II - Pole elektromagnetyczne, Warszawa, 1995, PWN.
- [2] Baron B., Piątek Ł.: Metody numeryczne w C++ Builder. Gliwice, Helion 2005
- [3] Sajdak C., Semek E.: Nagrzewanie indukcyjne. Podstawy teoretyczne i zastosowania. Wyd. Śląsk, Katowice 1987.
- [4] Baron B., Kolańska-Płuska J., Krych J.: Zastosowanie pewnej modyfikacji dyskretnej przekształcenia Fouriera do analizy harmonicznej pola elektromagnetycznego układów o symetrii obrotowej w C++. Materiały SPETO 2006, str. 53 – 56
- [5] Baron B., Kolańska-Płuska J., Krych J.: Zastosowanie dyskretnej przekształcenia Fouriera oraz algorytmu FFT w C++ do analizy pola elektromagnetycznego cewki z prądem. Materiały SPETO 2006, str. 49 – 52

Prof. dr hab. inż. Bernard Baron  
Silesian University of Technology, Poland  
ul. Akademicka 10, 44-100 Gliwice  
E-mail: bernard.baron@polsl.gliwice.pl  
Dr inż. Joanna Kolańska-Płuska  
Opole University of Technology, Poland  
ul. Luboszycka 7, 45-036 Opole  
E-mail: j.kolanska-pluska@po.opole.pl